

## ARTICLE OPEN



# Proteomics analysis of the gut–brain axis in a gut microbiota-dysbiosis model of depression

Yiyun Liu<sup>1,4</sup>, Haiyang Wang<sup>1,4</sup>, Siwen Gui<sup>1,4</sup>, Benhua Zeng<sup>2,4</sup>, Juncai Pu<sup>1,4</sup>, Peng Zheng<sup>1</sup>, Li Zeng<sup>1</sup>, Yuanyuan Luo<sup>1</sup>, You Wu<sup>1</sup>, Chanjuan Zhou<sup>1</sup>, Jinlin Song<sup>3</sup>, Ping Ji<sup>3</sup>, Hong Wei<sup>2</sup> and Peng Xie<sup>1</sup>

© The Author(s) 2021

Major depressive disorder (MDD) is a serious mental illness. Increasing evidence from both animal and human studies suggested that the gut microbiota might be involved in the onset of depression via the gut–brain axis. However, the mechanism in depression remains unclear. To explore the protein changes of the gut–brain axis modulated by gut microbiota, germ-free mice were transplanted with gut microbiota from MDD patients to induce depression-like behaviors. Behavioral tests were performed following fecal microbiota transplantation. A quantitative proteomics approach was used to examine changes in protein expression in the prefrontal cortex (PFC), liver, cecum, and serum. Then differential protein analysis and weighted gene coexpression network analysis were used to identify microbiota-related protein modules. Our results suggested that gut microbiota induced the alteration of protein expression levels in multiple tissues of the gut–brain axis in mice with depression-like phenotype, and these changes of the PFC and liver were model specific compared to chronic stress models. Gene ontology enrichment analysis revealed that the protein changes of the gut–brain axis were involved in a variety of biological functions, including metabolic process and inflammatory response, in which energy metabolism is the core change of the protein network. Our data provide clues for future studies in the gut–brain axis on protein level and deepen the understanding of how gut microbiota cause depression-like behaviors.

*Translational Psychiatry* (2021)11:568; <https://doi.org/10.1038/s41398-021-01689-w>

## INTRODUCTION

Major depressive disorder (MDD) is a serious mental illness characterized by low mood, loss of motivation, feelings of despair, and an inability to feel pleasure. MDD is one of the leading causes of disability worldwide [1], and >50% of patients do not remit after first-line antidepressant treatment despite numerous advances in the pharmacological treatment of depression [2]. Many studies have reported that depression is highly correlated with the activity of inflammatory signals [3, 4], alterations in neurotrophic signals [5], deficits in brain reward processing [6, 7], abnormal activity of the hypothalamic–pituitary–adrenal axis [8], changes in DNA methylation [9], and DNA damage [10]. However, these theories do not adequately explain the pathogenesis of depression. Interestingly, there is increasing evidence from both animal and human studies suggesting that the gut microbiota are actively involved in driving depression-like behaviors [11, 12] and provided new potential targets for MDD therapy [13].

Gut microbiota have been reported to regulate brain development, function, and behavior [14–16]. The use of germ-free (GF) mice maintained in a sterile environment allows assessment of how gut microbiota shape brain function and behavior. Bidirectional communication between the microbiota and brain via the gut–brain axis may contribute to the risk of neuropsychiatric diseases through alterations in the gastrointestinal system, central

nervous system, autonomic nervous system, and immune systems [14, 17]. Moreover, recent studies have confirmed profound effects of the microbiome on neuropsychiatric diseases such as autism spectrum disorder [18], schizophrenia [19], and Alzheimer's disease [20] via gut–brain axis.

In our previous clinical study, several altered metabolic byproducts of gut microbiota were found in urine of MDD patients, including hippurate, dimethylamine, and dimethylglycine [21]. We subsequently found that the gut microbial communities of MDD patients were significantly different from those of healthy controls [12], and these alternations were relatively specific compared to that observed in schizophrenia [22]. Moreover, based on a humanized fecal microbiota transplantation (FMT) animal model, we demonstrated that mice recipients of MDD fecal samples displayed depression-like behavior at 2 weeks post-transplantation and showed a significant disturbance of carbohydrate metabolism and amino acid metabolism compared with control mice [12]. We also found that gut microbiota caused molecular changes in multiple tissues, including the hippocampus, liver, cecum, serum, and hypothalamic–pituitary–adrenal axis [12, 23–25]. Mass spectrometry-based proteomics is a powerful approach to precisely quantify thousands of proteins in complex samples and to identify novel differentially expressed (DE) proteins between pathological states and controls [26, 27], which

<sup>1</sup>NHC Key Laboratory of Diagnosis and Treatment on Brain Functional Diseases, The First Affiliated Hospital of Chongqing Medical University, Chongqing, China. <sup>2</sup>Department of Laboratory Animal Science, College of Basic Medical Sciences, Third Military Medical University, Chongqing, China. <sup>3</sup>College of Stomatology, Chongqing Medical University, Chongqing, China. <sup>4</sup>These authors contributed equally: Yiyun Liu, Haiyang Wang, Siwen Gui, Benhua Zeng, Juncai Pu. ✉email: weihong63528@163.com; xiepeng@cqmu.edu.cn

Received: 27 July 2021 Revised: 17 October 2021 Accepted: 20 October 2021

Published online: 08 November 2021

has obvious advantages in discovering new targets and distinguishing psychiatric disorders [28, 29]. Thus, proteomics may be an effective way to reveal the underlying mechanisms of how the gut microbiota impact on hosts at the protein level.

The aim of this study was to capture the key protein alterations involved in the gut–brain axis. To this end, the gut microbiota of MDD patients was transplanted to GF mice. We then performed quantitative proteomics to examine the prefrontal cortex (PFC), liver, cecum, and serum. We hypothesized that gut microbiota would affect the host's gut–brain axis at the protein level and induce the depression-like behaviors.

## MATERIALS AND METHODS

### Animals

GF Kunming male mice (aged 6–8 weeks, weight 30–40 g) were obtained from the Experimental Animal Research Center of the Third Military Medical University (Chongqing, China). GF mice were kept in flexible film gnotobiotic isolators until the beginning of the behavioral tests. Mice were housed in standard autoclaved polypropylene cages with access to food and water ad libitum under a 12-h dark–light cycle (light on at 07:30) and at a constant temperature ( $23 \pm 1^\circ\text{C}$ ) and relative humidity ( $55\% \pm 5\%$ ). All animal handling and procedures followed the recommendations of the Guide for the Care and Use of Laboratory Animals and were approved by the Ethics Committee of Chongqing Medical University (Chongqing, China). Experimental and proteomics workflow of this study is shown in Fig. 1A.

### Fecal microbiota transplantation

Written informed consent was obtained from all participants. Participants aged 18–60 years were recruited from the psychiatric center and medical examination center of the First Affiliated Hospital of Chongqing Medical University. Eligible patients were drug-naïve with a primary diagnosis of MDD as assessed by the Structured Psychiatric Interview using Diagnostic and Statistical Manual of Mental disorder, Fourth Edition-Text Revision criteria [30] by an experienced psychiatrist. The score of 17-item Hamilton Depression Rating Scale of MDD patients were  $>18$  (mean [SD] score =  $26.8$  [4.0]). Exclusion criteria included a current diagnosis of physical or other mental disorders and substance abuse. Healthy controls were excluded if they had a history of neurological or other Axis I/II disorders, alcohol abuse or dependence, and illicit drug use. There were no differences in demographic characteristics between two groups. Fecal samples obtained from MDD patients ( $n = 5$ , 3 females, mean [SD] age =  $37.4$  [13.0]) and healthy controls ( $n = 5$ , 2 females, mean [SD] age =  $42$  [12.9]) were used to colonize the guts of GF mice. The protocol for microbiota transplantation was as previously described [12]. Briefly, fecal samples were collected under anaerobic conditions. We took 0.1 g of stool from each sample, then pooled five samples from the MDD or healthy group, respectively. The pooled 0.5 g of fecal sample for each group was suspended with 7.5 ml of 0.9% sterile phosphate-buffered saline to obtain suspension. GF mice were then randomly colonized with fecal samples from MDD patients or healthy controls in the flexible film gnotobiotic isolator.

### Behavioral testing

Two weeks after the FMT, the open field test (OFT) and the forced swim test (FST) for animals were performed within 2 days. After each individual test session, the apparatus was cleaned with 75% alcohol. All behavioral tests were recorded and analyzed by the EthoVision XT software (Noldus, Wageningen, Netherlands).

For the OFT, all mice were individually tested in an open-field apparatus ( $45 \times 45 \times 45$  cm). After 1 min of adaptation, all spontaneous activities were recorded for 5 min using a video tracking system [31]. For each animal, the total distance and percentage of time spent in the center quadrants were used to evaluate the anxiety-like behavior. For the FST, after 1 min of adaptation, all mice were individually placed into glass cylinders (30 cm high, 15 cm in diameter) containing 18 cm of water at  $23 \pm 2^\circ\text{C}$  for 5 min [32]. All sessions were recorded with a video tracking system. Immobility was defined as the least amount of movement needed to stay afloat. Duration of immobility were used to evaluate the depression-like behavior.

### Sample collection and preparation

After behavioral tests, the whole brain was rapidly removed, and PFC was dissected from the brain. Liver and cecum samples were also rapidly

obtained. All tissues were quick frozen in liquid nitrogen and then stored at  $-80^\circ\text{C}$ . Serum was immediately separated by centrifugation at 3000 rpm for 20 min at  $4^\circ\text{C}$  and then stored at  $-80^\circ\text{C}$ . Samples from 15 FMT-treated mice with depression-like phenotype and 15 control mice were prepared for proteome fractionation. The sample size was calculated by the power analysis with a Cohen's  $d$  effect size of 0.8. All tissues were homogenized in SDT buffer (4% SDS, 100 mM Tris-HCl, 1 mM DTT, pH 7.6) [33]. Proteins from five mice per group were pooled as a biological sample, and three biological replicates were obtained for each group. Proteins were digested with trypsin (Promega, Madison, WI, USA) in dissolution buffer overnight at  $37^\circ\text{C}$ . Peptides were purified on C18 Cartridges (Empore™ SPE Cartridges C18, bed I.D. 7 mm, volume 3 ml; Sigma, Steinheim, Germany), concentrated by vacuum centrifugation, and reconstituted in 0.1% (v/v) formic acid.

### iTRAQ labeling and strong cation exchanger (SCX)-based fractionation

The pooled samples were labeled using iTRAQ reagent according to the manufacturer's instructions (Applied Biosystems, Foster City, CA, USA). We used six tag of each iTRAQ 8-plex reagent ranging from 113 to 118. Four iTRAQ-labeling reagents were used for the 24 pools from the four tissues. iTRAQ-labeled peptides were fractionated by SCX chromatography using the AKTA Purifier system (GE Healthcare, Waukesha, WI, USA). The mixed iTRAQ-labeled samples were dissolved in buffer A (10 mM  $\text{KH}_2\text{PO}_4$  in 25% of ACN, pH 3.0) and were then eluted at a flow rate of 1 ml/min with a gradient of 0–8% buffer B (500 mM KCl, 10 mM  $\text{KH}_2\text{PO}_4$  in 25% of ACN, pH 3.0) for first 22 min, 8–52% buffer B from 23 to 47 min, 52–100% buffer B from 48 to 50 min, 100% buffer B from 51 to 58 min, and buffer B was reset to 0% after 58 min. The elution was monitored by absorbance at 214 nm, and fractions were collected every 1 min. For each experiment, 33 fractions were collected.

### Liquid chromatography tandem mass spectrometry (LC-MS/MS) and data analysis

Each fraction was injected for nano-LC and MS analysis. The peptide mixture were separated on a reverse phase trap column (Thermo Scientific Acclaim PepMap100,  $100 \mu\text{m} \times 2$  cm, nanoViper C18; Thermo Fisher Scientific, Waltham, MA, USA) connected to a C18-reversed phase analytical column (Easy column, 10 cm long, 75  $\mu\text{m}$  inner diameter, 3  $\mu\text{m}$  resin; Thermo Fisher Scientific, Waltham, MA, USA) in buffer A (0.1% formic acid) and then separated with a linear gradient of buffer B (84% acetonitrile and 0.1% formic acid) at a flow rate of 300 nl/min controlled by IntelliFlow technology. LC-MS/MS analysis was performed on a Q Exactive mass spectrometer outfitted with an Easy nLC (Thermo Scientific). The MS detection was survey scan (300–1800  $m/z$ ) with an target automated gain control value set of  $3e6$  and a maximum inject time of 10 ms. A dynamic exclusion time of 40 s was used. Survey scans were acquired at a resolution of 70,000 at  $m/z$  200, then the resolution for high-energy collisional dissociation spectra was set to 17,500 at  $m/z$  200, and isolation width was set to 2  $m/z$ .

Obtained MS/MS spectra were processed with Proteome Discoverer 1.4 (Thermo Fisher Scientific). The processed data were searched with Mascot version 2.2 (Matrix Science, London, UK). The mouse protein database was downloaded from Uniprot (released November 4, 2016) with 81,798 total entries. Two missed cleavages were allowed in fully and partially tryptic peptides. Carbamidomethyl (C), iTRAQ 8-plex (N-term), and iTRAQ 8-plex (K) were set as fixed modifications, and the oxidation (M) and iTRAQ 8-plex (Y) were set as variable modifications. The peptide mass tolerance was 20 ppm, and fragmentation tolerance was 0.1 Da. All peptide ratios were normalized by the median protein ratio. False discovery rate (FDR) were determined using a concatenated target-decoy database, and the peptides were identified with 1% FDR [34]. Proteins were considered to have differential abundance with a one-sample  $t$  test  $p$  value  $<0.05$  and a fold change  $>1.2$ .

### Statistical and bioinformatics analysis

All statistical tests were performed with the statistical software SPSS (version 17.0; Chicago, IL, USA). Kolmogorov–Smirnov and Shapiro–Wilk tests were used to assess the normality of the behavioral testing data and weight. Student's  $t$  test was performed to compare differences between the two groups. A  $p$  value  $<0.05$  was considered to indicate statistical significance. To further understand the similarities and differences of the detected proteins between the humanized FMT model and chronic stress

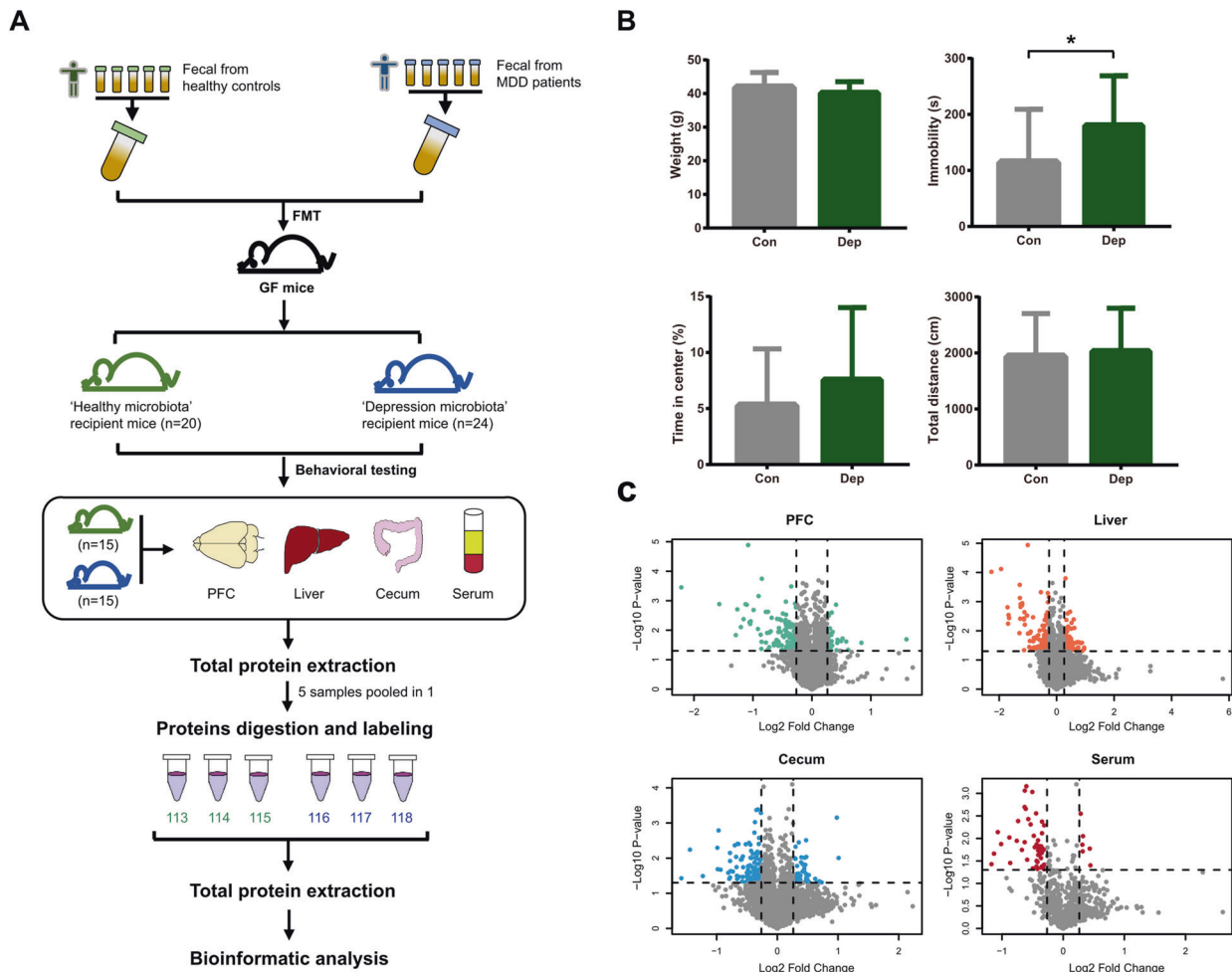


**Fig. 1** **Workflow of this study.** **A** Experimental and proteomics workflow of the study. **B** There were no differences in weight, total motion distance, and percentage of time spent in the center of the OFT between “depression microbiota” and “healthy microbiota” recipients. The “depression microbiota” recipients displayed an increased duration of immobility in the FST compared with “healthy microbiota” recipients (\* $p < 0.05$ ,  $t$  test). The gray bars indicate the “healthy microbiota” recipients ( $n = 20$ ). The green bars indicate the “depression microbiota” recipients ( $n = 24$ ). **C** Volcano plots of detected protein abundance from the four tissues. Green, orange, blue, and red dots indicate DE proteins in the PFC, liver, cecum, and serum, respectively.

models of depression, we compared the PFC data from the chronic social defeat stress (CSDS) model [35] and the liver data from chronic unpredictable mild stress (CUMS) model [36] reported in our previous studies. Moreover, we included our previous olfactory bulb (OB) data of FMT model in the bioinformatics analysis [37].

The protein datasets of different tissues were independently processed by weighted gene coexpression network analysis in the R software (version 3.6.1) [38]. We applied minimum module size to 20 proteins and the minimum height for merging modules at 0.25 to obtain the modules. Gene Ontology (GO) terms and models' overlap were performed by the Metascape [39]. Enrichment of GOs and DE proteins in modules were determined by Fisher's exact test corrected with Benjamini-Hochberg (BH) adjusted  $p$  value  $< 0.05$ . Protein annotation for functional groups and cellular compartment is obtained from the Ingenuity Pathway Analysis (IPA) software (QIAGEN Bioinformatics). Protein-protein interaction (PPI) networks were constructed by the STRING (version 11.0) and Cytoscape (version 3.7.2).

## RESULTS

### Changes in gut microbiota induced depression-like behaviors

Two weeks after FMT, behavioral tests were performed to evaluate whether gut microbiota affected the function of the brain. There was no significant difference in body weight between the two groups ( $t = 1.34$ ,  $p = 0.19$ ; Fig. 1B). In the OFT, there were no

differences in the total distance or percentage of time spent in the center between the “depression microbiota” recipient mice and control mice ( $t = -0.42$ ,  $p = 0.68$ ;  $t = -1.30$ ,  $p = 0.20$ ). In the FST, the immobility time of “depression microbiota” recipient mice was significantly increased compared with controls ( $t = -2.38$ ,  $p = 0.02$ ). These results were consistent with our previous studies [12, 25], suggesting that disturbances of gut microbiota affect behaviors.

### Protein expression profile of gut-brain axis

Large-scale protein analysis was performed on the PFC, liver, cecum, and serum from two groups. We identified 27,445 unique peptides in the PFC with an FDR  $< 1\%$ , covering 4846 proteins. With the same parameters, a total of 4858 proteins (29,096 unique peptides) were identified in the liver, 4167 proteins (22,036 unique peptides) in the cecum, and 848 proteins (4504 unique peptides) in serum (Tables S1–S4). All identified proteins of four tissues showed a large range of abundance, and the distributions of proteins varied among tissues (Fig. 1C).

Analysis of protein location and functional annotation by IPA revealed that protein location of serum was different from the other three tissues (Fig. 2A and Tables S5–S8). All proteins were assigned to 13 functional groups (Fig. 2B). We found that the proportion of various functional proteins detected in the cecum and liver was

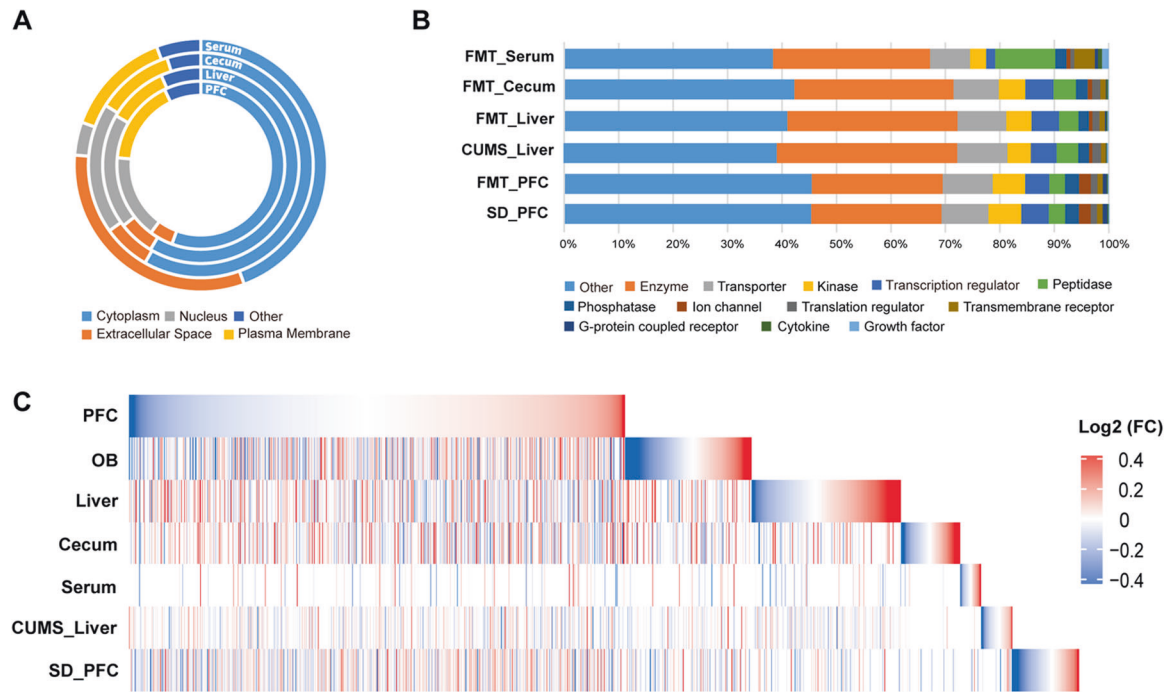


**Fig. 2 Protein expression profile.** **A** Donut plots represent the percentages of cellular compartments of all proteins. **B** Composition of the functional groups annotated by IPA. In the PFC, about 2.1% of proteins involved in ion channel functions, which was approximately twice as high as that in the liver, cecum, and serum. The proportion of G protein-coupled receptors in the PFC was also three times higher than that in the cecum and liver. In the serum, the numbers of growth factors, cytokines, transmembrane receptors, and peptidases were markedly higher than that in the other three tissues. **C** Union heatmaps show fold changes of all proteins for the gut–brain axis of FMT model, the PFC of CSDS model, and the liver of CUMS model.

similar, but it was different between the PFC and serum (Fig. 2B). Further, the union heatmap of protein expression levels showed obvious separations among the four tissues (Fig. 2C).

In order to further reveal the similarities and differences of the detected proteins between the humanized FMT model and chronic stress models of depression, we compared the data of PFC from the humanized FMT model and CSDS model and the data of liver from humanized FMT model and CUMS model. In general, 67.1% of PFC proteins of FMT model overlapped with CSDS model, and 55.8% of liver proteins of FMT model overlapped with CUMS model (Fig. S1A). However, only 1.9 and 1.1% of DE proteins of FMT model overlapped with CSDS and CUMS models, respectively (Fig. S1B). For the same tissue from different models, the protein expression showed divergence, indicating that microbiota-driven protein changes were different from the chronic stress.

### Comparisons of differential protein expression among tissues

We identified 159, 187, 148, and 55 DE proteins in the PFC, liver, cecum, and serum, respectively (Tables S1–S4). Further, the majority of DE proteins were downregulated (Fig. S2A). There were no DE proteins that overlapped in all four tissues (Fig. S2B). Five DE proteins overlapped between the PFC and cecum, and six overlapped between the liver and cecum. For brain tissues, PFC and OB shared ten DE proteins as well. These results suggested that gut microbiota exerted different impact on multiple tissues of the gut–brain axis.

### Coexpression analysis identified microbiota-related protein modules

To assess the proteome-wide changes among tissues of gut–brain axis in a more comprehensive manner, we constructed independent protein coexpression networks based on all detected proteins from five tissues. We identified 21, 29, 17, 19, and 9 coexpression modules in the PFC (P1–P21 modules), OB (O1–O29 modules), liver (L1–L17 modules), cecum (C1–C17 modules), and

serum (S1–S9 modules), respectively (Fig. S3), ranging from 22 to 1631 proteins. In total, 18 modules were enriched for DE proteins in the gut–brain axis, which were considered as microbiota-related modules (FDR < 0.05, Fig. 3A). The circus plot of these modules suggested that the microbiota-related modules across the gut–brain axis showed similar protein expression (Fig. 3B).

To examine the biological function of the microbiota-related modules, we conducted GO enrichment analysis (Fig. 3C). These modules were extensively involved in the metabolic process, including small molecule catabolic process (adjusted  $p = 0.002$ ), cellular modified amino acid metabolic process (adjusted  $p = 0.007$ ), drug metabolic process (adjusted  $p < 0.001$ ), and dicarboxylic acid metabolic process (adjusted  $p < 0.001$ ). Modules of PFC and OB were involved in inflammatory response to antigenic stimulus (adjusted  $p < 0.001$ ). Notably, L2, C18, O29, P3, and P20 were all enriched in the cellular respiration (adjusted  $p < 0.001$ ) and oxidative phosphorylation (adjusted  $p < 0.001$ ), which are critical energy metabolism pathways.

Further, we constructed the PPI networks based on the DE proteins of the gut–brain axis (Fig. S4) and annotated the protein functions by GO. In the PPI networks of PFC and cecum, proteins involved in the energy metabolism formed separate subnetworks (Fig. 4A, C). In the OB and liver, energy metabolism-relevant proteins showed a tight link and played important roles in the structure of the entire PPI networks (Fig. 4B, D). Together, these results suggested that DE proteins were highly enriched in energy metabolism across tissues of gut–brain axis and might have worked in a synergistic way.

### DISCUSSION

Increasing evidence supports that gut microbiota are important contributors to the balance between mental health and disease [13]. In the present study, a humanized FMT model was used to induce depression-like behavior, and an iTRAQ-based quantitative

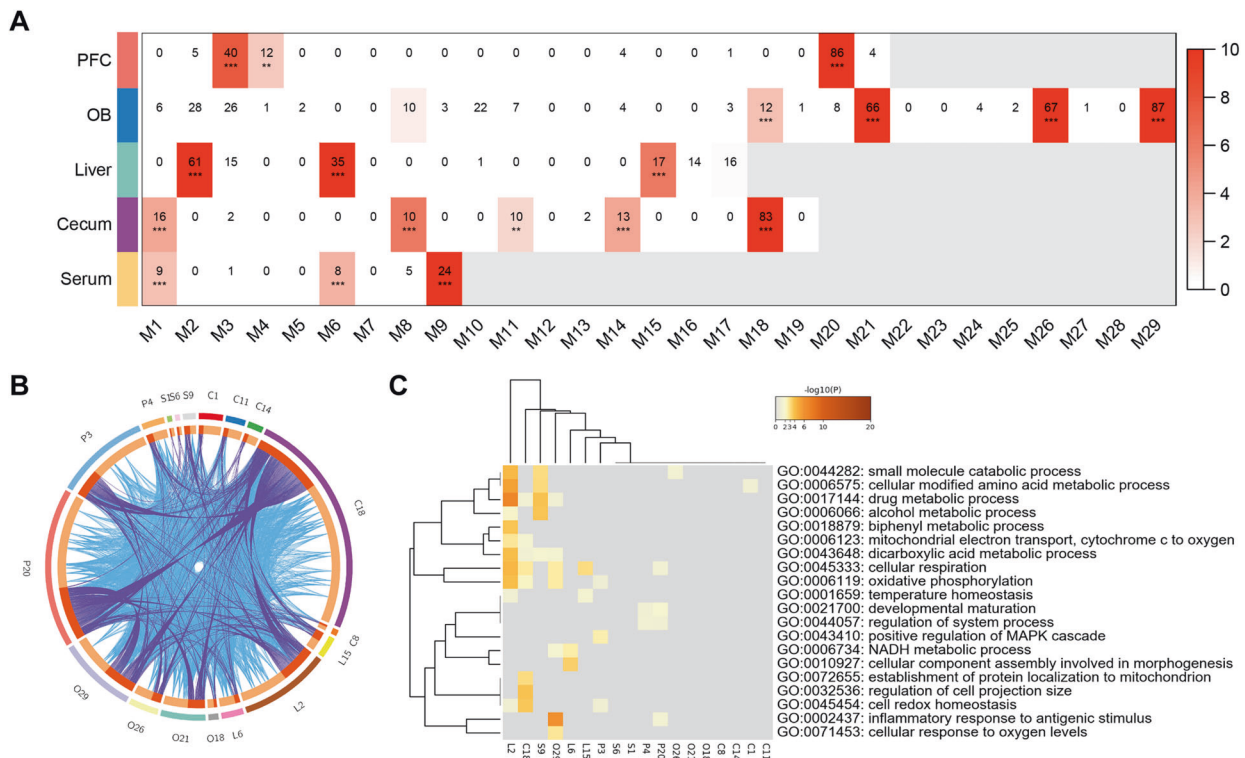


**Fig. 3 DE proteins and microbiota-related coexpression modules.** **A** Matrix summarizes enrichment of DE proteins in coexpression modules for each tissue. The significance of enrichment ( $-\log_{10}$  (BH-corrected  $p$  value), one-sided Fisher's exact test) is scaled by color intensity. BH-corrected  $**p < 0.01$ ,  $***p < 0.001$ . **B** Circos plot shows overlapped proteins in modules from PFC, OB, liver, cecum, and serum. The outside arcs of circos plot represent each module, and the inside arcs represent the proteins in each module. Dark orange represents the proteins that appear in multiple module and light orange represents proteins that are unique to that module. Purple links indicate the overlapped proteins among modules, and blue links indicate the functional overlap among modules. **C** GO enrichment analysis for 18 microbiota-related modules. The heatmap cells are colored by the  $p$  values of representative GO terms.

proteomics approach was used to explore protein expression of the gut-brain axis. Our results supported that gut microbiota induced altered protein expression levels in multiple tissues of the gut-brain axis in mice with depression-like phenotype, and these changes of the PFC and the liver showed to be model specific. In addition, protein changes of the gut-brain axis were involved in a variety of biological functions, including metabolic process and inflammatory response, in which energy metabolism is the core change of protein networks.

As is well known, the gut microbiota can modulate host's functions in energy uptake, storage, and expenditure. Microbes can increase energy harvest through the short-chain fatty acids produced by fermentation [40]. We found that the gut microbiota not only changed the energy metabolism of cecum but also had profound effect on the PFC, OB, and liver. Moreover, our model is based on the GF mice, and these gut-brain axis protein changes involved in energy metabolism may be a cause of depression-like behaviors, rather than a consequence. This suggests that the effect of gut microbiota could transmit from intestinal tract to brain. These findings are consistent with previous studies which showed that the altered gut microbiota could impact the host's metabolism [12, 40, 41]. Besides, increasing preclinical studies suggested that the gut microbiota might induce depression-like phenotype via the vagus nerve [42, 43] and the subdiaphragmatic vagotomy blocked behavioral changes in knockout mice treated with an antibiotic cocktail [44, 45].

Metabolomics studies have revealed that depression patients showed disturbance of energy metabolism both in urine and plasma [21, 46]. In a proteomics study, postmortem dorsolateral PFC brain tissue of patients with MDD showed significant differences in energy metabolism [47]. Our previous study found

that the liver of the FMT-treated mice with depression-like phenotype also presented energy metabolism change on metabolite level [24]. In a transcriptomic study, depression-like behaviors were accompanied with mitochondrial energy metabolism as well [48]. These studies on multiple molecular types supported that depression was closely related to energy metabolism.

Our results showed that 5-hydroxytryptamine receptor 2A (HTR2A), a member of the serotonin receptor family, was significantly upregulated in the PFC of mice with depression-like phenotype, which is consistent with clinical studies of MDD patients [49–51]. HTR2A is highly associated with depression severity and plays an important role in the serotonin signaling pathway of depression [52]. Most of the body's 5-HT are produced in the gut and regulates its movement. Gut microbiota were reported to regulate host's 5-HT and physiology via the colonic enterochromaffin cells [53]. The gut-driven 5-HT alteration could lead to abnormal liver gluconeogenesis and glucose uptake through HTR2B [54]. These data indicated that gut microbiota might alter the expression of neurotransmitters in the brain to influence the behaviors.

Based on the comparison of datasets, we found that over half of detected proteins in the humanized FMT model overlapped with chronic stress models; however, only approximately 1–2% of DE proteins overlapped between these models. The DE proteins of the humanized FMT model differed markedly from the chronic stress models of depression in both PFC and liver. These results suggested that microbiota might have a novel pathogenic mechanism, which differed from common psychological and physical stress. Moreover, previous studies reported that the depression-like mice of CSDS model showed a distinct microbiota

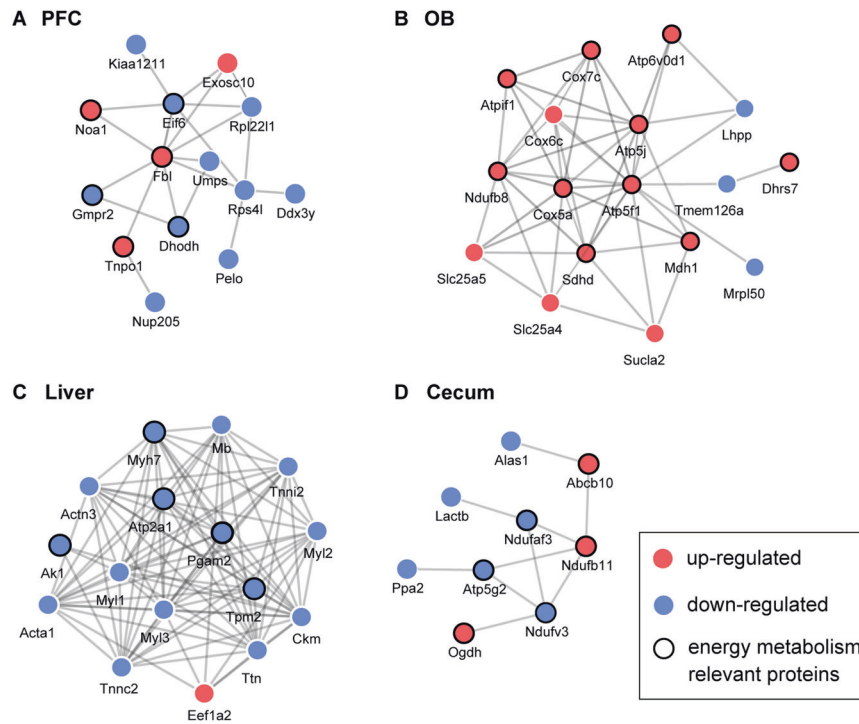


**Fig. 4** The PPI networks of the gut–brain axis. The PPI network of the **A** PFC, **B** liver, **C** cecum, and **D** serum based on the DE proteins. Blue dots indicate downregulated DE proteins. Red dots indicate upregulated DE proteins.

composition compared with controls [55]. Further, the depression-like Flinders sensitive line rats, which are used as an experimental animal model of depression, showed lower bacterial richness and altered relative abundance of several bacterial phyla [56]. These studies suggested that the onset of depression often followed with alterations in microbiota composition. Based on the FMT model of depression, our data demonstrate that depressive-like phenotypes can be transmitted from human to mice.

Our study had several limitations. First, we used male GF mice to construct the humanized depression model. Nevertheless, other studies showed that females were 2–3 times more likely to develop MDD and suffered greater functional impairment [57, 58]. Besides, although GF mice showed limitation in development and immunity [59], they are still valuable for exploring whether or not gut microbiota impact a given process [60]. Therefore, the future studies using female GF mice and antibiotics-treated mice can provide a supplement to our results. Moreover, as all recipient mice were kept in flexible film gnotobiotic isolators characterized by a higher interior air pressure to avoid potential contamination of forage and air, we did not perform the sucrose preference test, a measurement for the behavior of anhedonia that is a core symptom of MDD [61]. Also, our behavioral tests were performed out of the isolators, and it is necessary to explore the effect of short-term air exposure on the composition of gut microbiota in subsequent experiments. In addition, only four tissues related to the brain–gut axis were investigated in our study, while changes in microbiota were also reported to affect other tissues, including the heart and pancreas [62, 63].

In conclusion, using a gut microbiota-dysbiosis model of depression, we found that gut microbiota may have an essential role in the development of depression-like behaviors and contribute to changes of the protein expression and functions of the gut–brain axis, especially the energy metabolism. Our data provide clues for future studies on the gut–brain axis at the protein level and deepen the understanding of how gut microbiota cause depression-like behaviors.

## REFERENCES

- Global Burden of Disease Study 2013 Collaborators. Global, regional, and national incidence, prevalence, and years lived with disability for 301 acute and chronic diseases and injuries in 188 countries, 1990–2013: a systematic analysis for the Global Burden of Disease Study 2013. *Lancet*. 2015;386:743–800.
- Carvalho AF, Berk M, Hyphantis TN, McIntyre RS. The integrative management of treatment-resistant depression: a comprehensive review and perspectives. *Psychother Psychosom*. 2014;83:70–88.
- Bierhaus A, Wolf J, Andrassy M, Rohleder N, Humpert PM, Petrov D, et al. A mechanism converting psychosocial stress into mononuclear cell activation. *Proc Natl Acad Sci USA*. 2003;100:1920–5.
- Mostafavi S, Battle A, Zhu X, Potash JB, Weissman MM, Shi J, et al. Type I interferon signaling genes in recurrent major depression: increased expression detected by whole-blood RNA sequencing. *Mol Psychiatry*. 2014;19:1267–74.
- Marshall J, Zhou XZ, Chen G, Yang SQ, Li Y, Wang Y, et al. Antidepressant action of BDNF requires and is mimicked by Galphai1/3 expression in the hippocampus. *Proc Natl Acad Sci USA*. 2018;115:E3549–58.
- Rea E, Rummel J, Schmidt TT, Hadar R, Heinz A, Mathe AA, et al. Anti-anhedonic effect of deep brain stimulation of the prefrontal cortex and the dopaminergic reward system in a genetic rat model of depression: an intracranial self-stimulation paradigm study. *Brain Stimul*. 2014;7:21–8.
- Krishnan V, Nestler EJ. The molecular neurobiology of depression. *Nature*. 2008;455:894–902.
- Saaltink DJ, Vreugdenhil E. Stress, glucocorticoid receptors, and adult neurogenesis: a balance between excitation and inhibition? *Cell Mol Life Sci*. 2014;71:2499–515.
- Ho AM, Winham SJ, Armasu SM, Blacker CJ, Millischer V, Lavebratt C, et al. Genome-wide DNA methylomic differences between dorsolateral prefrontal and temporal pole cortices of bipolar disorder. *J Psychiatry Res*. 2019;117:45–54.
- Ceylan D, Yilmaz S, Tuna G, Kant M, Er A, Ildiz A, et al. Alterations in levels of 8-Oxo-2'-deoxyguanosine and 8-Oxoguanine DNA glycosylase 1 during a current episode and after remission in unipolar and bipolar depression. *Psychoneuroendocrinology*. 2020;114:104600.
- Kelly JR, Borre Y, O'Brien C, Patterson E, El Aidy S, Deane J, et al. Transferring the blues: Depression-associated gut microbiota induces neurobehavioural changes in the rat. *J Psychiatry Res*. 2016;82:109–18.
- Zheng P, Zeng B, Zhou C, Liu M, Fang Z, Xu X, et al. Gut microbiome remodeling induces depressive-like behaviors through a pathway mediated by the host's metabolism. *Mol Psychiatry*. 2016;21:786–96.
- Sharon G, Sampson TR, Geschwind DH, Mazmanian SK. The central nervous system and the gut microbiome. *Cell*. 2016;167:915–32.

14. Fung TC, Olson CA, Hsiao EY. Interactions between the microbiota, immune and nervous systems in health and disease. *Nat Neurosci*. 2017;20:145–55.
15. Sampson TR, Mazmanian SK. Control of brain development, function, and behavior by the microbiome. *Cell Host Microbe*. 2015;17:565–76.
16. Cryan JF, Dinan TG. Mind-altering microorganisms: the impact of the gut microbiota on brain and behaviour. *Nat Rev Neurosci*. 2012;13:701–12.
17. Foster JA, McVey Neufeld KA. Gut-brain axis: how the microbiome influences anxiety and depression. *Trends Neurosci*. 2013;36:305–12.
18. Hsiao EY, McBride SW, Hsien S, Sharon G, Hyde ER, McCue T, et al. Microbiota modulate behavioral and physiological abnormalities associated with neurodevelopmental disorders. *Cell*. 2013;155:1451–63.
19. Severance EG, Gressitt KL, Stallings CR, Origoni AE, Khushalani S, Leweke FM, et al. Discordant patterns of bacterial translocation markers and implications for innate immune imbalances in schizophrenia. *Schizophr Res*. 2013;148:130–7.
20. Wu SC, Cao ZS, Chang KM, Juang JL. Intestinal microbial dysbiosis aggravates the progression of Alzheimer's disease in *Drosophila*. *Nat Commun*. 2017;8:24.
21. Zheng P, Wang Y, Chen L, Yang D, Meng H, Zhou D, et al. Identification and validation of urinary metabolite biomarkers for major depressive disorder. *Mol Cell Proteomics*. 2013;12:207–14.
22. Zheng P, Zeng B, Liu M, Chen J, Pan J, Han Y, et al. The gut microbiome from patients with schizophrenia modulates the glutamate-glutamine-GABA cycle and schizophrenia-relevant behaviors in mice. *Sci Adv*. 2019;5:eaa8317.
23. Huo R, Zeng B, Zeng L, Cheng K, Li B, Luo Y, et al. Microbiota modulate anxiety-like behavior and endocrine abnormalities in hypothalamic-pituitary-adrenal axis. *Front Cell Infect Microbiol*. 2017;7:489.
24. Li B, Guo K, Zeng L, Zeng B, Huo R, Luo Y, et al. Metabolite identification in fecal microbiota transplantation mouse livers and combined proteomics with chronic unpredictable mild stress mouse livers. *Transl Psychiatry*. 2018;8:34.
25. Zeng L, Zeng B, Wang H, Li B, Huo R, Zheng P, et al. Microbiota modulates behavior and protein kinase C mediated cAMP response element-binding protein signaling. *Sci Rep*. 2016;6:29998.
26. Aebersold R, Mann M. Mass spectrometry-based proteomics. *Nature*. 2003;422:198–207.
27. Cravatt BF, Simon GM, Yates JR 3rd. The biological impact of mass-spectrometry-based proteomics. *Nature*. 2007;450:991–1000.
28. Cabello-Arreola A, Ho AM, Ozerdem A, Cuellar-Barboza AB, Kucuker MU, Heppelmann CJ, et al. Differential dorsolateral prefrontal cortex proteomic profiles of suicide victims with mood disorders. *Genes*. 2020;11:256.
29. Ho AM, Cabello-Arreola A, Markota M, Heppelmann CJ, Charlesworth MC, Ozerdem A, et al. Label-free proteomics differences in the dorsolateral prefrontal cortex between bipolar disorder patients with and without psychosis. *J Affect Disord*. 2020;270:165–73.
30. American Psychiatric Association. *Diagnostic and Statistical Manual of Mental Disorders, 4th Edition-Text Revision*. Washington, DC: APA; 2000.
31. Kim CS, Chang PY, Johnston D. Enhancement of dorsal hippocampal activity by knockdown of HCN1 channels leads to anxiolytic- and antidepressant-like behaviors. *Neuron*. 2012;75:503–16.
32. Oury F, Khirimian L, Denny CA, Gardin A, Chamouni A, Goeden N, et al. Maternal and offspring pools of osteocalcin influence brain development and functions. *Cell*. 2013;155:228–41.
33. Zhu Y, Xu H, Chen H, Xie J, Shi M, Shen B, et al. Proteomic analysis of solid pseudopapillary tumor of the pancreas reveals dysfunction of the endoplasmic reticulum protein processing pathway. *Mol Cell Proteomics*. 2014;13:2593–603.
34. Elias JE, Gibbons FD, King OD, Roth FP, Gygi SP. Intensity-based protein identification by machine learning from a library of tandem mass spectra. *Nat Biotechnol*. 2004;22:214–9.
35. Guo H, Huang ZL, Wang W, Zhang SX, Li J, Cheng K, et al. iTRAQ-based proteomics suggests Ephb6 as a potential regulator of the ERK pathway in the prefrontal cortex of chronic social defeat stress model mice. *Proteomics Clin Appl*. 2017. <https://doi.org/10.1002/prca.201700115>.
36. Wu Y, Tang J, Zhou C, Zhao L, Chen J, Zeng L, et al. Quantitative proteomics analysis of the liver reveals immune regulation and lipid metabolism dysregulation in a mouse model of depression. *Behav Brain Res*. 2016;311:330–9.
37. Huang C, Yang X, Zeng B, Zeng L, Gong X, Zhou C, et al. Proteomic analysis of olfactory bulb suggests CACNA1E as a promoter of CREB signaling in microbiota-induced depression. *J Proteomics*. 2019;194:132–47.
38. Zhang B, Horvath S. A general framework for weighted gene co-expression network analysis. *Stat Appl Genet Mol Biol*. 2005;4:Article17.
39. Zhou Y, Zhou B, Pache L, Chang M, Khodabakhshi AH, Tanaseichuk O, et al. Metascape provides a biologist-oriented resource for the analysis of systems-level datasets. *Nat Commun*. 2019;10:1523.
40. Heiss CN, Olofsson LE. Gut microbiota-dependent modulation of energy metabolism. *J Innate Immun*. 2018;10:163–71.
41. Cox LM, Yamanishi S, Sohn J, Alekseyenko AV, Leung JM, Cho I, et al. Altering the intestinal microbiota during a critical developmental window has lasting metabolic consequences. *Cell*. 2014;158:705–21.
42. Wang S, Ishima T, Zhang J, Qu Y, Chang L, Pu Y, et al. Ingestion of *Lactobacillus intestinalis* and *Lactobacillus reuteri* causes depression- and anhedonia-like phenotypes in antibiotic-treated mice via the vagus nerve. *J Neuroinflammation*. 2020;17:241.
43. Zhang J, Ma L, Chang L, Pu Y, Qu Y, Hashimoto K. A key role of the subdiaphragmatic vagus nerve in the depression-like phenotype and abnormal composition of gut microbiota in mice after lipopolysaccharide administration. *Transl Psychiatry*. 2020;10:186.
44. Pu Y, Tan Y, Qu Y, Chang L, Wang S, Wei Y, et al. A role of the subdiaphragmatic vagus nerve in depression-like phenotypes in mice after fecal microbiota transplantation from Chrn7 knock-out mice with depression-like phenotypes. *Brain Behav Immun*. 2021;94:318–26.
45. Wang S, Ishima T, Qu Y, Shan J, Chang L, Wei Y, et al. Ingestion of *Faecalibaculum rodentium* causes depression-like phenotypes in resilient Ephx2 knock-out mice: a role of brain-gut-microbiota axis via the subdiaphragmatic vagus nerve. *J Affect Disord*. 2021;292:565–73.
46. Zheng P, Gao HC, Li Q, Shao WH, Zhang ML, Cheng K, et al. Plasma metabolomics as a novel diagnostic approach for major depressive disorder. *J Proteome Res*. 2012;11:1741–8.
47. Martins-de-Souza D, Guest PC, Harris LW, Vanattou-Saifouline N, Webster MJ, Rahmoune H, et al. Identification of proteomic signatures associated with depression and psychotic depression in post-mortem brains from major depression patients. *Transl Psychiatry*. 2012;2:e87.
48. Xie X, Shen Q, Yu C, Xiao Q, Zhou J, Xiong Z, et al. Depression-like behaviors are accompanied by disrupted mitochondrial energy metabolism in chronic corticosterone-induced mice. *J Steroid Biochem Mol Biol*. 2020;200:105607.
49. McMahon FJ, Buervenich S, Charney D, Lipsky R, Rush AJ, Wilson AF, et al. Variation in the gene encoding the serotonin 2A receptor is associated with outcome of antidepressant treatment. *Am J Hum Genet*. 2006;78:804–14.
50. Yatham LN, Liddle PF, Sossi V, Erez J, Vafai N, Lam RW, et al. Positron emission tomography study of the effects of tryptophan depletion on brain serotonin(2) receptors in subjects recently remitted from major depression. *Arch Gen Psychiatry*. 2012;69:601–9.
51. Marinova Z, Monoranu CM, Fetz S, Walitza S, Grunblatt E. Region-specific regulation of the serotonin 2A receptor expression in development and ageing in post mortem human brain. *Neuropathol Appl Neurobiol*. 2015;41:520–32.
52. Smith RM, Papp AC, Webb A, Ruble CL, Munsie LM, Nisenbaum LK, et al. Multiple regulatory variants modulate expression of 5-hydroxytryptamine 2A receptors in human cortex. *Biol Psychiatry*. 2013;73:546–54.
53. Yano JM, Yu K, Donaldson GP, Shastri GG, Ann P, Ma L, et al. Indigenous bacteria from the gut microbiota regulate host serotonin biosynthesis. *Cell*. 2015;161:264–76.
54. Sumara G, Sumara O, Kim JK, Karsenty G. Gut-derived serotonin is a multifunctional determinant to fasting adaptation. *Cell Metab*. 2012;16:588–600.
55. Yang C, Fujita Y, Ren Q, Ma M, Dong C, Hashimoto K. Bifidobacterium in the gut microbiota confer resilience to chronic social defeat stress in mice. *Sci Rep*. 2017;7:45942.
56. Tillmann S, Abildgaard A, Winther G, Wegener G. Altered fecal microbiota composition in the Flinders sensitive line rat model of depression. *Psychopharmacology*. 2019;236:1445–57.
57. Kessler RC, Chiu WT, Demler O, Merikangas KR, Walters EE. Prevalence, severity, and comorbidity of 12-month DSM-IV disorders in the National Comorbidity Survey Replication. *Arch Gen Psychiatry*. 2005;62:617–27.
58. Kornstein SG, Schatzberg AF, Thase ME, Yonkers KA, McCullough JP, Keitner GI, et al. Gender differences in chronic major and double depression. *J Affect Disord*. 2000;60:1–11.
59. Kennedy EA, King KY, Baldrige MT. Mouse microbiota models: comparing germ-free mice and antibiotics treatment as tools for modifying gut bacteria. *Front Physiol*. 2018;9:1534.
60. Cryan JF, O'Riordan KJ, Cowan CSM, Sandhu KV, Bastiaanssen TFS, Boehme M, et al. The microbiota-gut-brain axis. *Physiol Rev*. 2019;99:1877–2013.
61. Liu MY, Yin CY, Zhu LJ, Zhu XH, Xu C, Luo CX, et al. Sucrose preference test for measurement of stress-induced anhedonia in mice. *Nat Protoc*. 2018;13:1686–98.
62. Tang WH, Kitai T, Hazen SL. Gut microbiota in cardiovascular health and disease. *Circ Res*. 2017;120:1183–96.
63. Ahuja M, Schwartz DM, Tandon M, Son A, Zeng M, Swaim W, et al. Ora1-mediated antimicrobial secretion from pancreatic acini shapes the gut microbiome and regulates gut innate immunity. *Cell Metab*. 2017;25:635–46.

#### AUTHOR CONTRIBUTIONS

PX and HW conceived and designed the project. Y Liu, PZ, LZ, CZ, JS, and PJ conducted the experiments. SG and JP performed bioinformatics. HW, BZ, Y Luo, and

YW performed FMT mice model. Y Liu and PX wrote the manuscript. All the authors contributed to the manuscript.

### FUNDING INFORMATION

This project was supported by grants from the National Key Research and Development Program of China (2017YFA0505700), the Non-profit Central Research Institute Fund of Chinese Academy of Medical Sciences (2019PT320002), the Natural Science Foundation Project of China (81820108015 and 82101596), and the China Postdoctoral Science Foundation (2020M673160). The funders had no role in study design, data collection and analysis, decision to publish, or preparation of the manuscript.

### COMPETING INTERESTS

The authors declare no competing interests.

### ADDITIONAL INFORMATION

**Supplementary information** The online version contains supplementary material available at <https://doi.org/10.1038/s41398-021-01689-w>.

**Correspondence** and requests for materials should be addressed to Hong Wei or Peng Xie.

**Reprints and permission information** is available at <http://www.nature.com/reprints>

**Publisher's note** Springer Nature remains neutral with regard to jurisdictional claims in published maps and institutional affiliations.



**Open Access** This article is licensed under a Creative Commons Attribution 4.0 International License, which permits use, sharing, adaptation, distribution and reproduction in any medium or format, as long as you give appropriate credit to the original author(s) and the source, provide a link to the Creative Commons license, and indicate if changes were made. The images or other third party material in this article are included in the article's Creative Commons license, unless indicated otherwise in a credit line to the material. If material is not included in the article's Creative Commons license and your intended use is not permitted by statutory regulation or exceeds the permitted use, you will need to obtain permission directly from the copyright holder. To view a copy of this license, visit <http://creativecommons.org/licenses/by/4.0/>.

© The Author(s) 2021